Internal Report
DESY M 10-02
May 2010

Influences of a Beam-Pipe Discontinuity on the Signals of a Nearby Beam Position Monitor (BPM)

A.K. Bandyopadhyay, A. Joestingmeier, A.S. Omar, R. Wanzenberg

Deutsches Elektronen-Synchrotron DESY, Hamburg

Internal Report
DESY M 10-02
May 2010

Influences of a beam-pipe discontinuity on the signals of a nearby beam position monitor (BPM)

A.K. Bandyopadhyay [*], A. Joestingmeier, A.S. Omar
Otto-von-Guericke University, Magdeburg, Germany.

R. Wanzenberg
DESY, Hamburg, Germany.

Abstract

The aim of this study is to investigate the influences of a discontinuity in the beam pipe on the signals picked up by a nearby beam position monitor (BPM). In this investigation a simple button type BPM with a coaxial output port has been considered. A groove in the beam pipe has been considered as a typical discontinuity. The electromagnetic simulation softwares MAFIA and Microwave Studio have been used for the electromagnetic field computations.

Geometry and parameters of the considered problem

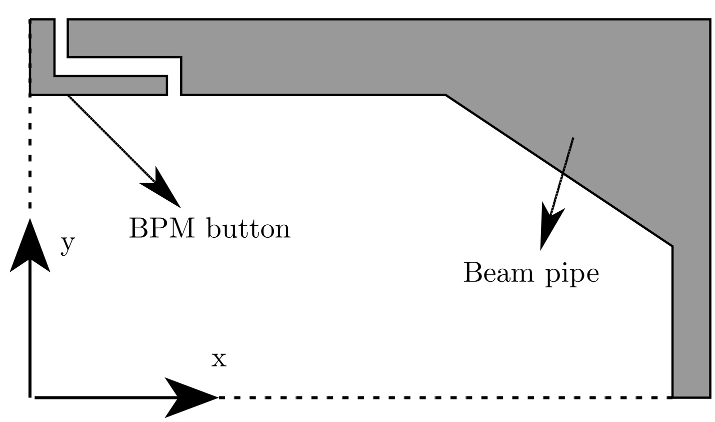

Figure 1: Schematic diagram (xy plane) of the beam pipe with the BPM button.

Figs. 1 and 2 show the schematic diagrams of the geometry considered for the simulations. Fig. 1 shows the cross section of the beam pipe, while Fig. 2 illustrates the corresponding

[*] Presently working in the ESRF, Grenoble, France.

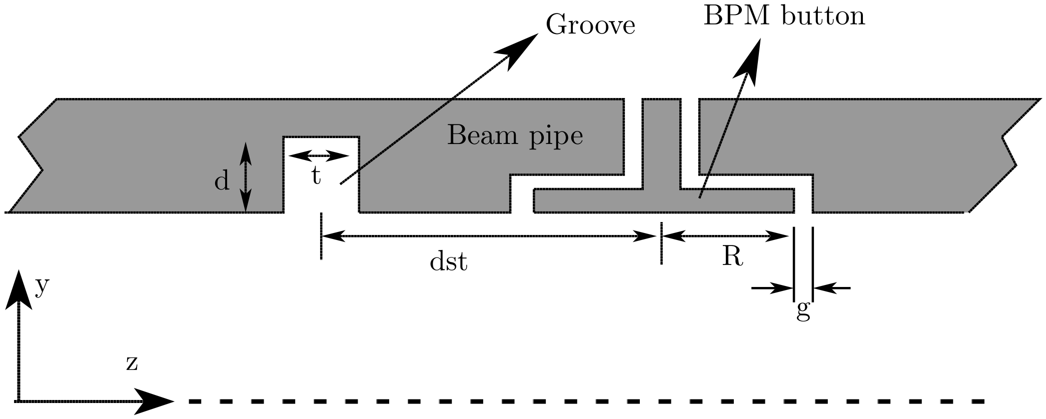

Figure 2: Schematic diagram (yz plane) of the beam pipe with the BPM button and groove.

longitudinal section. In order to reduce the required memory for the field computations, a simplified BPM geometry has been considered. The symmetry of the structure enables us to further reduce the memory requirement. Besides the BPM geometry Fig. 2 also shows the groove, which has been considered as the discontinuity. The distance between the centers of the groove and the BPM button (dst), the width (t) and depth (d) of the groove, the radius of the BPM button (R) etc. as shown in Fig. 2 can be considered as the main parameters for the considered problem.

Simulation Results

Parameters used for the simulation

To start with, a BPM with a button radius (R) of 5.0 mm has been considered. The groove has been considered to be mounted at distances (dst) of 20.0 mm, 40.0 mm and 80.0 mm from the center of the BPM button. The depth (d) and width (t) of the groove have been considered to be 5.0 mm and 2.0 mm respectively. The gap between the BPM button and the beam pipe (g) has been assumed to be 0.6 mm. All of these parameters have been shown in Fig. 2. A uniform beam pipe with a length of 15.0 mm has been considered before the groove and after the BPM button, i.e. at both sides of the discontinuities. The width and height of the beam pipe have been taken as 40 mm and 20 mm, respectively. The dimensions of the inner and outer conductor of the coaxial line have been chosen such that the impedance of the coaxial port is very near to 50 Ohm. In order to asses the results correctly, the structure with the same meshing scheme but without the groove has been considered for each case.

Scattering parameter

The three dimensional geometry of the structure under consideration is shown in Fig. 3. One-quarter of the test structure can be seen, along with one half of the BPM button and the

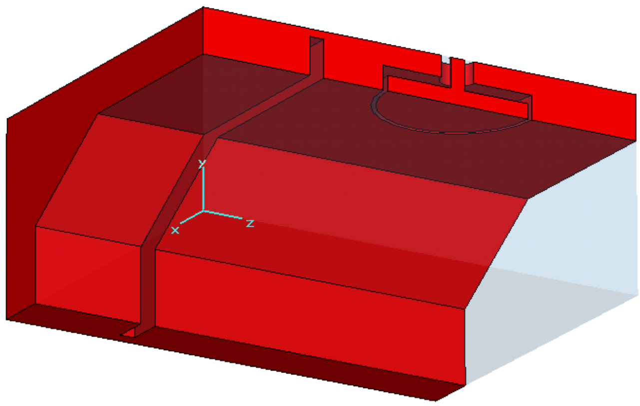

Figure 3: The beam-pipe along with the groove and the beam position monitor.

coaxial port. Due to the symmetry of the structure, only one quarter is needed to be modeled in case of excitation through an on-axis beam.

To confirm the consistency of the model and meshing, some scattering parameters of the considered structure have been computed using Microwave Studio [1] and MAFIA [2]. It may be noted that MAFIA is able to compute the wake fields [3, 4] as well as the coaxial port output signals due to charged bunch excitations [5, 6, 7]. For the scattering parameter computations, the coaxial port has been used as the excitation port and the beam pipe has been terminated with short circuits at the two extreme z-boundaries. The electric field pattern of the fundamental coaxial port mode which has been used for the excitations is shown in Fig. 4. For the scattering parameter computation, a full reflection of the input signal has been recorded at the coaxial port. The full reflection is due to the short circuits at the both z-boundaries of the structure. The comparison between the computed phases of the reflection coefficients (versus frequency) between the Microwave Studio and the MAFIA model is shown in Fig. 5. Here it may be noted that the meshing with Microwave Studio has been created using the expert meshing system for automatic mesh generation. This expert meshing system generates the mesh based on the defined geometrical details of the structure. For the MAFIA simulations a manual meshing has been used. However, the excellent agreement between the results from both softwares confirms the consistency of the manual meshing used with MAFIA.

Wake computation

In the next step the wake field computations have been done for a particle bunch with Gaussian charge distribution passing through the center of the structure. The rms bunch length (σ_z) has been considered as 10.0 mm. The mesh step size along the z-direction for the wake computations (which is required to be uniform along z direction) has been taken as 0.2 mm. In the x- and in the y- directions near the groove and the BPM button, a finer mesh size of 0.1 mm has been used. The three dimensional MAFIA model of the structure and the mesh details near the BPM button are shown in Fig. 6. Three sets of wake computations have

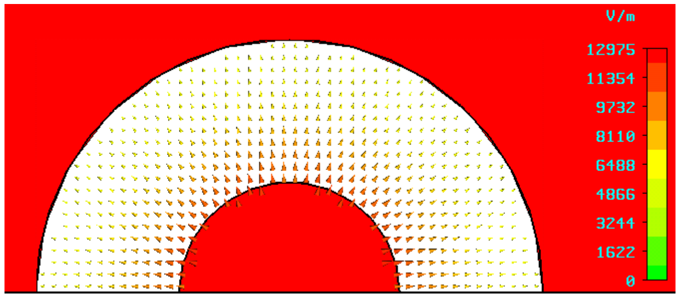

Figure 4: Electric field pattern for the coaxial port mode.

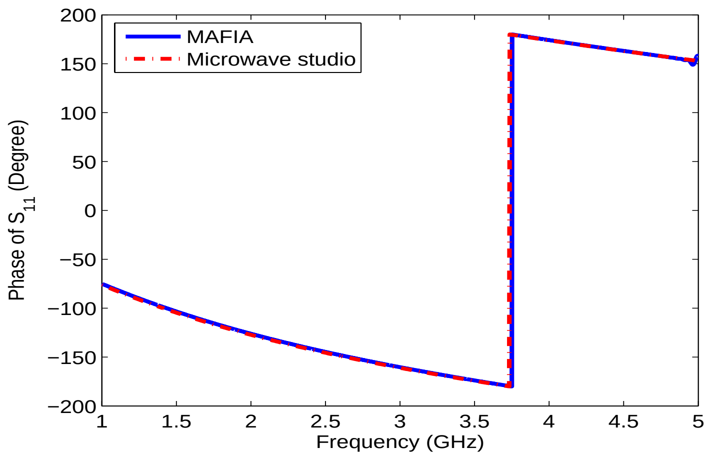

Figure 5: Comparison between the phases of the reflection coefficient (s_{11}) at the coaxial waveguide port of the test structure computed with Microwave Studio and MAFIA.

been done assuming three different positions of the groove with respect to the BPM button. The distance (dst) between the BPM button and the groove has been measured as shown in Fig. 2. The distances for which BPM signals have been computed are 20.0 mm, 40.0 mm and 80.0 mm, respectively. The comparisons of the recorded BPM signal at the coaxial port with and without the groove for each three cases are shown in Figs 7, 9 and 10, respectively. Although there is not much noticeable difference between the two recorded signals in Fig. 7, a closer inspection revels the difference between them. A detailed plot around the first peak of the recorded signals is shown in Fig. 8. It can be noted here, that similar situations are also found for the two other cases. It can be noted here that the recorded signals in Fig. 7 and Figs. 9 and 10 show opposite polarities. This is because of the opposite polarities of the port-mode electric field distributions used to record the output signals. The absolute values of the differences between the recorded BPM signals with and without the groove for these three cases are plotted in Figs. 11(a), 11(b) and 11(c) respectively. It can be seen that for the considered cases, the obtained results does not vary from each other significantly.

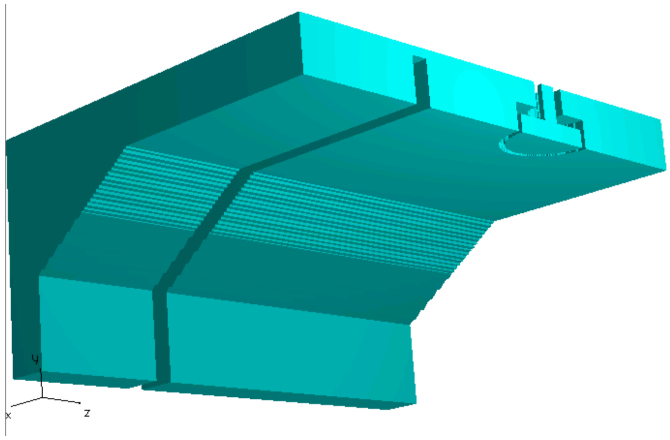

(a) Three dimensional MAFIA model of the beam pipe with the groove and BPM button.

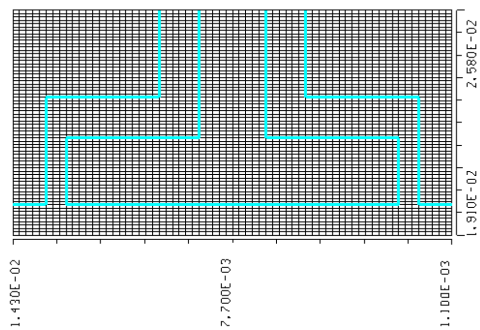

(b) Details of meshing near the BPM button.

Figure 6: The three dimensional MAFIA model and details of meshing used for the wakefield computations.

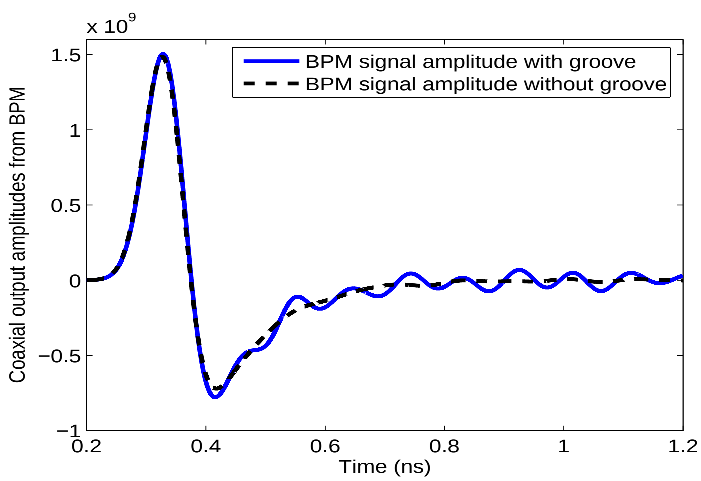

Figure 7: Comparison between the output wave amplitudes at the coaxial port with and without the groove. The distance between the groove and the button is 20.0 mm.

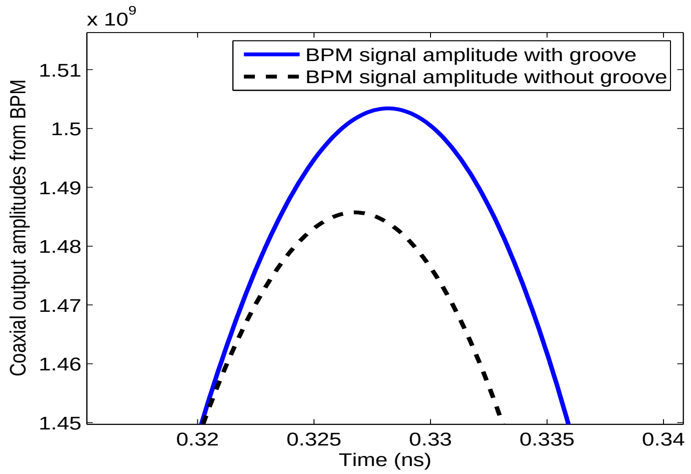

Figure 8: Details of the difference between the recorded BPM signals shown in Fig. 7 with and without the groove at a distance of 20 mm from the button.

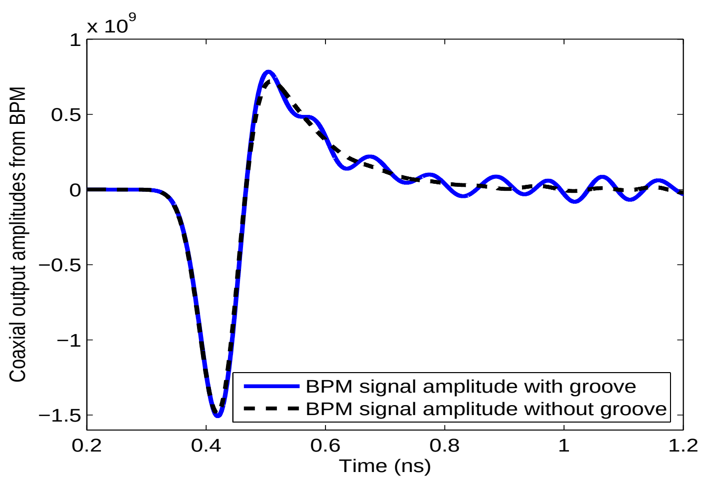

Figure 9: Comparison between the output wave amplitudes at the coaxial port with and without the groove. The distance between the groove and the button is 40.0 mm.

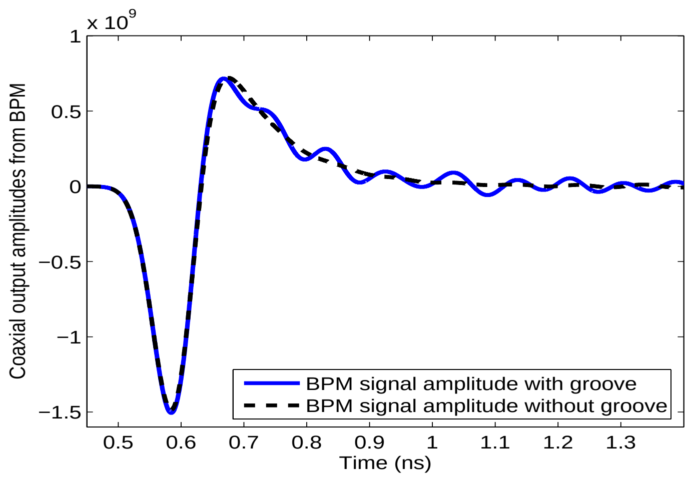

Figure 10: Comparison between the output wave amplitudes at the coaxial port with and without the groove. The distance between the groove and the button is 80.0 mm.

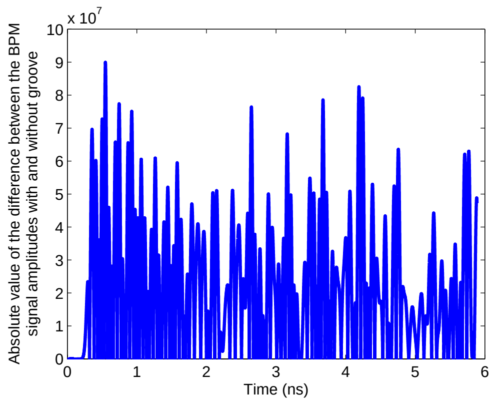

(a) dst = 20.0 mm

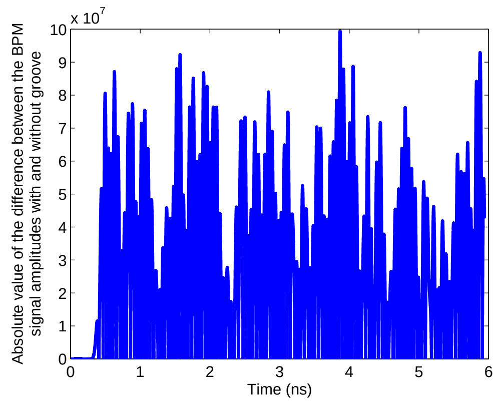

(b) dst = 40.0 mm

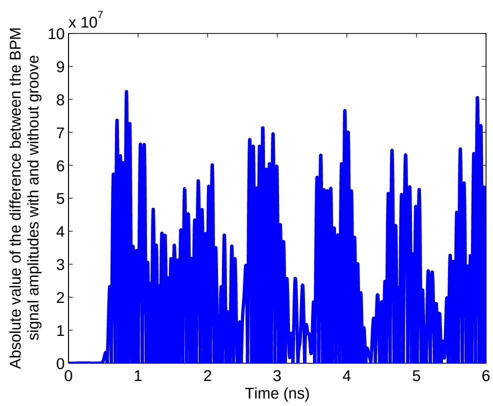

(c) dst = 80.0 mm

Figure 11: Absolute values of the difference between the recorded coaxial output signals versus time for three different distances between the groove and the button (dst).

Analysis of the BPM signals

In order to study the influence of the groove in the frequency domain, the Discrete Fourier Transform has been used. By comparing the frequency domain responses with and without the groove, the influences of the groove can be analyzed. Fig. 12 shows the comparisons of the output signals at the coaxial port in the time and frequency domain with and without groove. From Fig. 12 it can be observed that the frequency response of the coaxial output signal for the beam pipe with groove contains some sharp peaks at certain frequencies, whereas that without the groove is smooth.

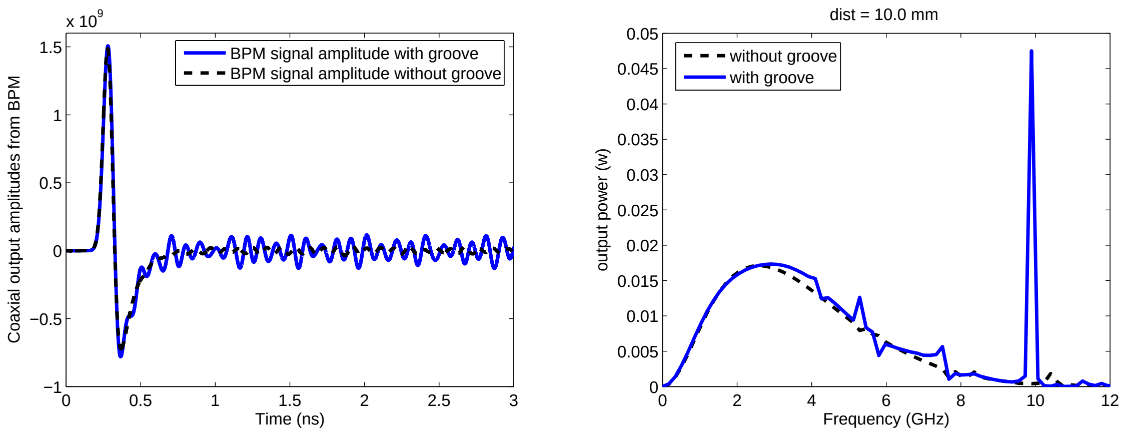

(a) Output signal at the coaxial port in time domain. (b) Output signal at the coaxial port in frequency domain.

Figure 12: Output signal at the coaxial port in the time and the frequency domain for a distance of 10 mm between the groove and the BPM.

The total energy coming out of the coaxial port due to a circulating particle bunch inside the beam pipe can be calculated from the BPM signals. As the time taken by a particle bunch to circulate once along the machine (the revolution period) is much larger than the transient duration of the BPM signal, this energy can be computed by an integration with respect to time over the output power at the coaxial port. This quantity is the total energy coming out of the output coaxial port per revolution of the beam. If the output signal recorded at the coaxial port in the time domain is denoted by $S(t)$, the total energy can be computed as,

$$E_{tot} = \int |S(t)|^2 dt \tag{1}$$

Similarly one can calculate the energy output in the frequency domain. It may be noted that $S(t)$ depends linearly on the total charge of the circulating bunch. Therefore, for a bunch with total charge Q_{bunch} the normalized energy output E_{norm} can simply be defined as,

$$E_{norm} = \frac{E_{tot}}{Q_{bunch}^2} \tag{2}$$

Distance between the groove and BPM center (mm)	Normalized output energy at the coaxial port (V/C)		Difference between the energy outputs with and without groove
	With groove	Without groove	
10	1.8038×10^8	1.5562×10^8	15.9%
20	1.6497×10^8	1.5498×10^8	6.45%
40	1.6862×10^8	1.5516×10^8	8.67%
80	1.6162×10^8	1.5483×10^8	4.39%

Table 1: Normalized energies coming out of the coaxial ports for different cases.

The total energy coming out of the coaxial port [eq. (1)] due to an 1 nC exciting bunch comes out to be 1.5562×10^{-10} J. This result has been cross checked by computing it from the frequency domain data, yielding the same outcome. The normalized energies coming out of the coaxial port [eq. (1)-(2)] for all the considered cases with and without groove have been shown in Table 1. From the table it can be seen that the output energy remains almost constant for the cases without the groove, as expected. With presence of the groove, the differences between the output energies vary between 4.4% to 16%, depending on the distance from the groove. However, these differences may vary sharply if any resonant mode having significant coupling between the groove and the BPM is present.

In order to investigate the reason of the sharp peaks in the output signal spectra, an eigenmode analysis has been done. From the eigenmode analysis, the resonant frequencies (up to 11 GHz) of the considered structure have been computed. To compute the modes concentrated near the BPM button, the two extreme z-boundaries have been terminated once with electrical walls and once with magnetic walls. The computed resonant frequencies of the structure are listed in Table 2. From the table, it can be seen that the resonant frequency of the first resonant mode is not influenced by the termination of the z-boundaries. The electric field distribution shows that this mode is totally confined near the BPM button. The two- and three-dimensional electric field distribution for the mode are shown in Fig. 13. From the frequency spectrum of the BPM signal (Fig. 12), it can be seen that there are no spike near the resonant frequency of this trapped mode. So it can be inferred that the excitation through a on-axis beam has almost no coupling to this mode. The spikes of the output signal are caused due to the other resonant modes of the structure and the groove, which could possibly be excited by the beam.

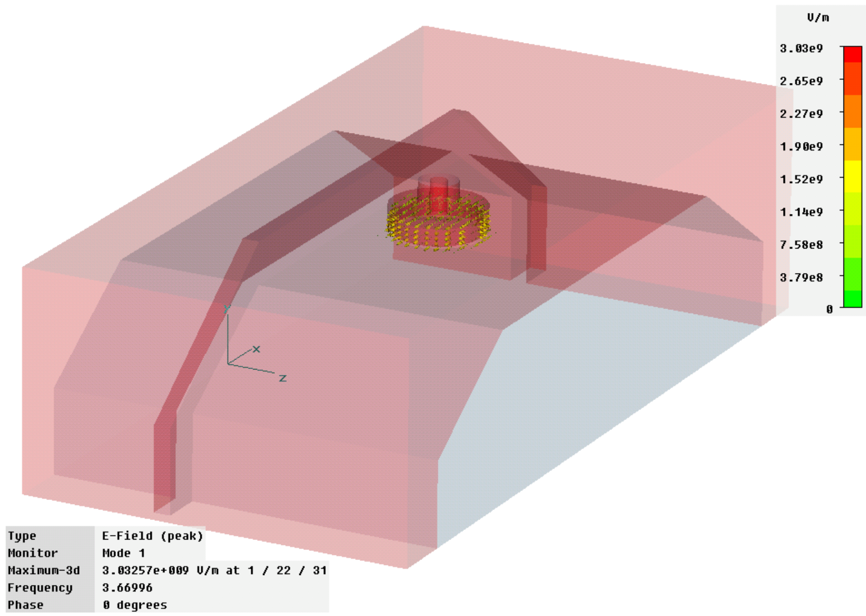

(a) Three dimensional electric field distribution of the mode near the BPM button.

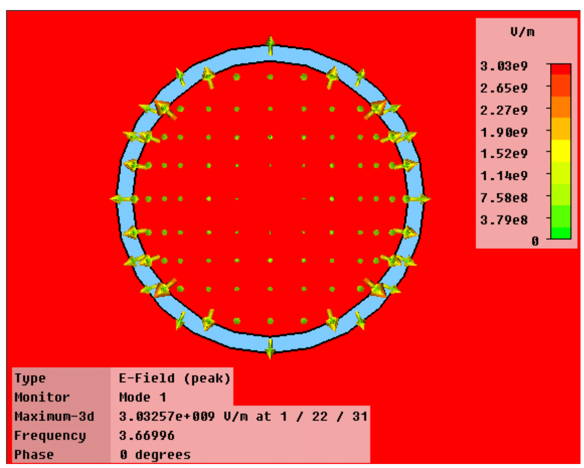

(b) Two dimensional electric field distribution of the mode near the BPM button.

Figure 13: Electric field distribution of the mode concentrated near the BPM button with the resonant frequency 3.67 GHz.

Mode no.	Resonant frequencies (GHz)	
	Magnetic walls at z-boundaries	Electric walls at z-boundaries
1	3.67	3.66
2	4.81	4.21
3	5.23	5.32
4	5.77	5.79
5	7.57	6.97
6	7.63	7.62
7	7.67	7.70
8	7.99	8.00
9	8.29	8.31
10	9.40	9.45
11	9.93	9.92
12	-	9.94

Table 2: Resonant frequencies of the beam pipe with a groove and BPM, with different boundary conditions at the z-boundaries. The distance between the groove and the BPM button is 10 mm.

In order to investigate the reason of the spikes in the output signal spectra, the same structure has been modeled without the BPM. Instead of the BPM, three electric field monitors have been used to record the time domain fields. The excitation has been provided by a Gaussian bunch with total charge of 1 C, as previously. Three field monitors have been used to record the electric field (x-component) during the whole time domain computation. The structure as modeled in MAFIA along with the positions of the three electric field monitors is shown in Fig. 15. The first two monitors have been placed inside the groove whereas the third one has been placed at the position of the BPM center. The time variation of the electric field (x-components) recorded at these three positions are shown in Fig. 14. The corresponding frequency spectrum of these electric field components are shown in Fig. 16. From Fig. 16(a), it can be seen that there are sharp resonance peaks around 5.8, 7.6, 8.0 and 9.9 GHz. Among these resonance peaks, the strongest one appears at 9.9 GHz. A sharp resonance at this

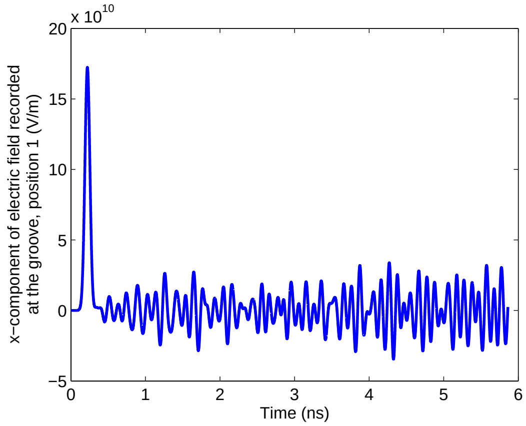

(a) Electric field (x-component) at position 1.

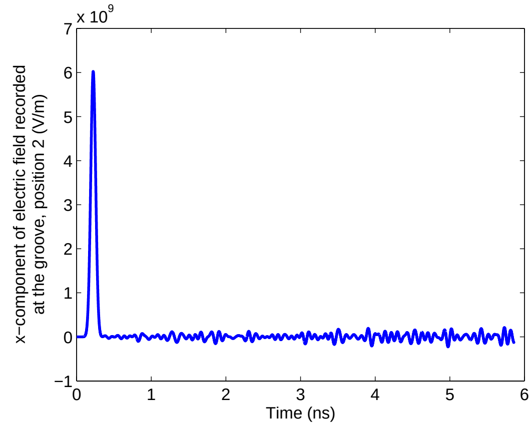

(b) Electric field (x-component) at position 2.

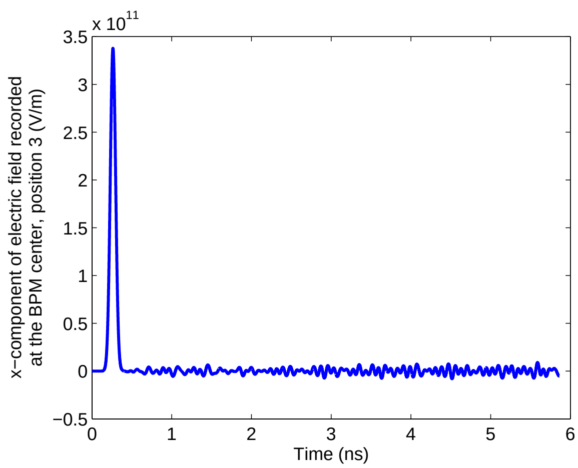

(c) Electric field (x-component) at position 3.

Figure 14: Electric fields (x component) recorded at the positions 1, 2 and 3 (Fig. 15)

frequency can also be seen in the output spectrum of the BPM signal (Fig. 12(b)). So it can be concluded that the sharp peak at 9.9 GHz in the BPM output signal spectrum is due to a resonant mode near the groove, which has a considerable coupling to the BPM. A couple of modes have been found with the eigenmode computations (once with electric wall and once with magnetic wall at the z-boundaries) which have such field distributions. The electric field distribution of such a mode is shown in Fig. 17. This is the mode number 11 of Table 2 (electric walls at z-boundaries).

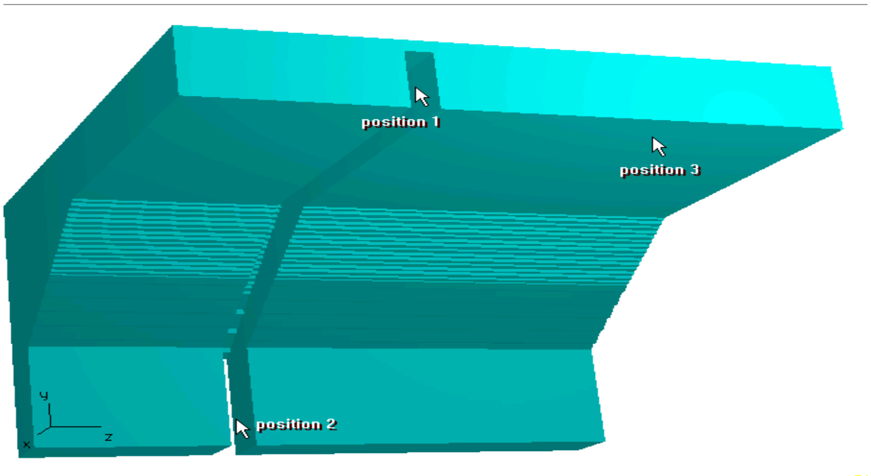

Figure 15: Position of the electric field monitors used in the MAFIA simulations.

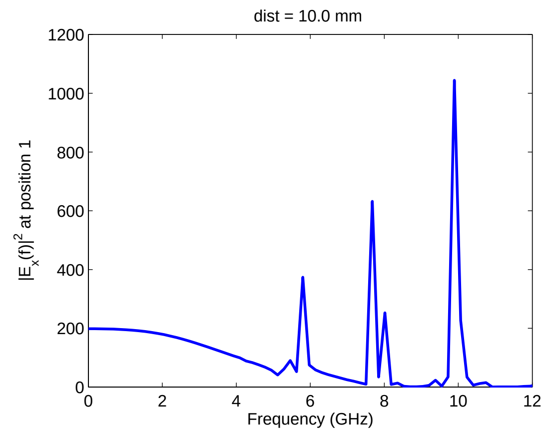

(a) Frequency spectrum of the electric field (x-component) at position 1.

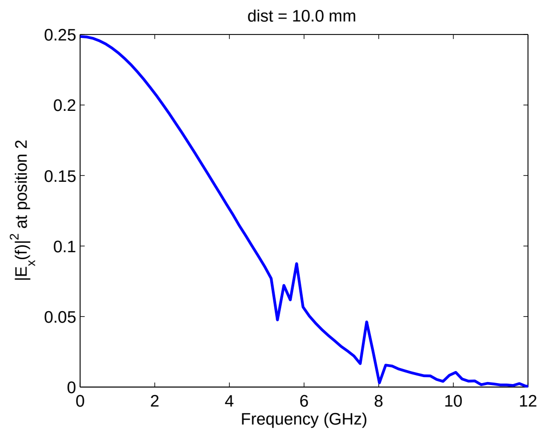

(b) Frequency spectrum of the electric field (x-component) at position 2.

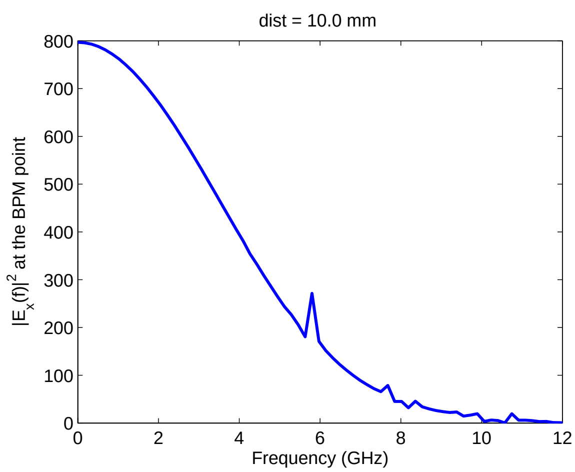

(c) Frequency spectrum of the electric field (x-component) at position 3.

Figure 16: Frequency spectrum of the electric fields (x-component) recorded at the positions 1, 2 and 3 (Fig. 15)

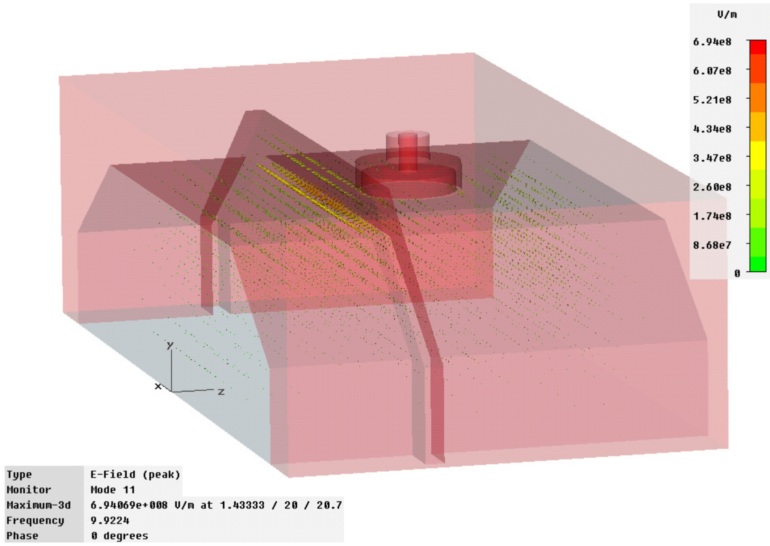

Figure 17: Electric field distribution of the 11-th mode showing a considerable coupling between the groove and the BPM.

Excitation by an off-axis beam

For the computations in case of excitation through an off-axis beam, one half of the beam pipe with two output coaxial waveguide ports has been modeled. To investigate the influence of the groove, the beam pipe has been modeled once with the groove and once without it.

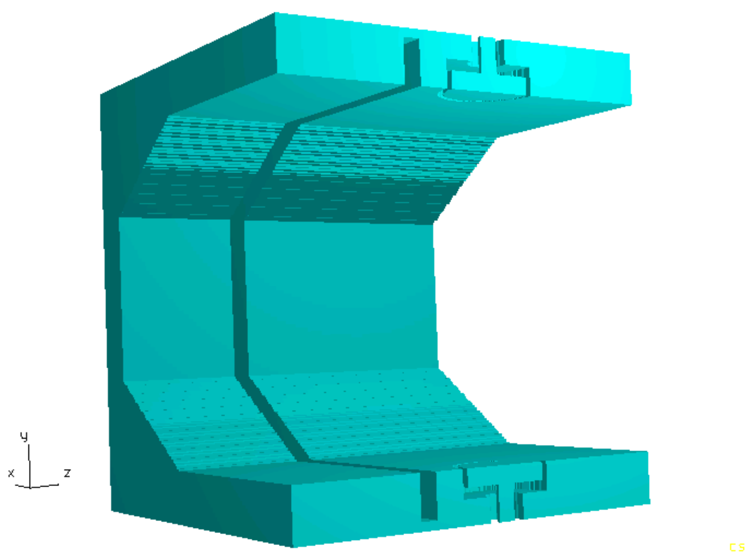

Figure 18: Beam pipe with the BPM and groove for the simulations with off-axis beam.

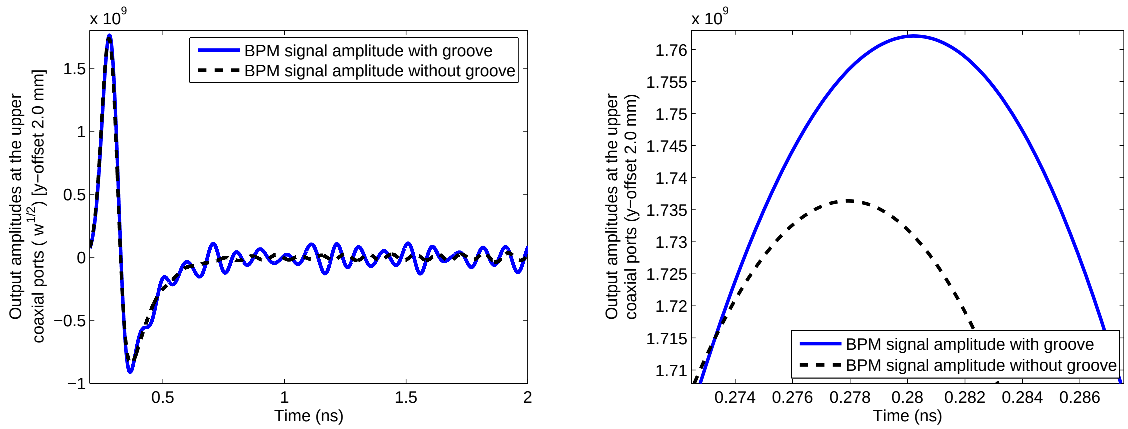

(a) Output signal recorded at the upper coaxial port with and without groove.

(b) Details of the output signal recorded at the upper coaxial port with and without groove.

Figure 19: Output signal at the upper coaxial port for a beam with 2.0 mm y-offset.

Both on- and off-axis cases have been computed. The characteristics of the excitation has been kept the same as before, i.e. a Gaussian bunch with a total charge of 1 C. The modeled structure (with MAFIA) can be seen in Fig. 18. A y-offset of 2.0 mm has been considered for the computations and the distance between the groove and the BPM is considered as 10 mm. The comparison of the output wave amplitudes recorded at the upper coaxial port is shown in Fig. 19. Comparing the case of the considered on-axis beam (Figs. 7 and 8) with the present one, it can be noticed that the difference between the output signals (with and without groove) remains almost in the same range for the offset and the on-axis beam. The frequency spectrums of the coaxial output signals for the off-axis case with and without the groove are shown in Fig. 20. Comparing Figs. 12(b) and 20 one can note that there are no significant difference in the output signal spectrums except small differences in the signal amplitudes.

Another case has been considered with a 10 mm y-offset of the beam. Both the cases (with and without the groove) have been considered. Fig. 21 shows comparison of the output signals recorded at the upper coaxial port. The corresponding signal spectrum in frequency domain is shown in Fig. 22(a). In the frequency spectrum, no significant change has been found except for the spike near 10 GHz. The differences between the output signal amplitudes

y-offset	Normalized energy output at the coaxial port (V/C)					
	With groove			Without groove		
(mm)	Upper coax	Lower coax	Total	Upper coax	Lower coax	Total
0.0	1.80×10^8	1.80×10^8	3.61×10^8	1.56×10^8	1.56×10^8	3.12×10^8
2.0	2.39×10^8	1.38×10^8	3.77×10^8	2.12×10^8	1.14×10^8	3.26×10^8
10.0	8.93×10^8	5.7×10^7	9.50×10^8	8.39×10^8	2.84×10^7	8.67×10^8

Table 3: Output energies from the coaxial ports for the beam pipe with and without grooves with different y-offsets of the beam.

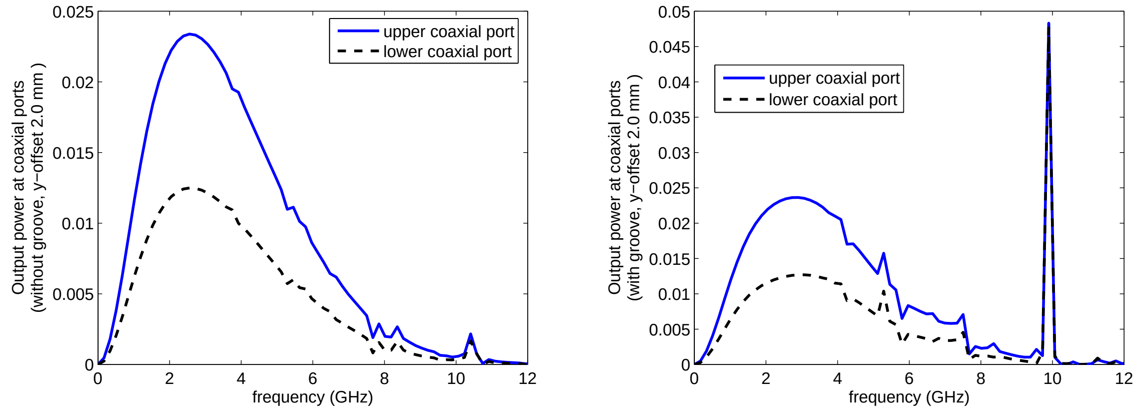

(a) Output signal spectrum at the coaxial ports without groove.

(b) Output signal spectrum at the coaxial ports with groove.

Figure 20: Output signal spectrums at the upper coaxial port for a beam with 2.0 mm y-offset.

with and without the groove for the cases of on-axis beam, 2 mm y-offset beam and 10 mm y-offset beam are 2.18×10^7, 2.57×10^7 and 5.24×10^7 $\sqrt{\text{Watt}}$ respectively, corresponding to a bunch with 1 C charge. The normalized output energy at the coaxial ports for different cases calculated according to equations [(1)-(2)] are summarized in Table 3.

The signals picked up by the BPM buttons are used to determine the position of the beam inside the beam pipe. Usually a normalized ratio of the BPM signals are used for this purpose. If the we denote the signals coming out of the upper and lower coaxial ports as S_U and S_L, respectively, we can define this normalized ratio R as,

$$R = \frac{S_U - S_L}{S_U + S_L} \tag{3}$$

The deviation in the value of R with and without the groove indicates the error in determining the beam position due to the discontinuity (groove). The ratio R calculated with the help of eq. (3) for the two y-offsets are summarized in Table 4.

y-offset (mm)	Calculated ratio R [eq. (3)]		Difference in R with and without groove
	with groove	without groove	
0	0	0	-
2	0.268	0.301	12.21%
10	0.880	0.935	6.20%

Table 4: The ratio R calculated according to eq. (3) for different vertical offsets with and without the groove. The distance between the groove and the BPM button is 10 mm.

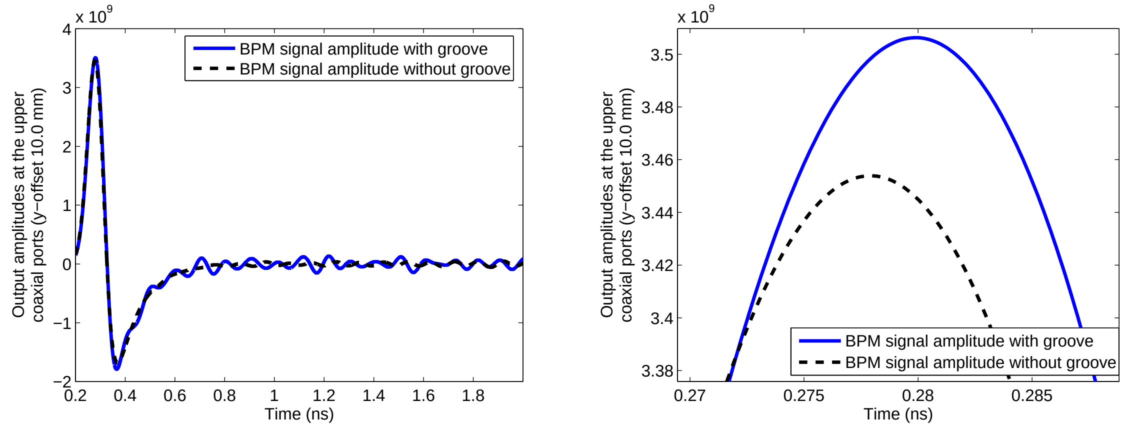

(a) Output signal recorded at the upper coaxial port with and without groove.

(b) Details of the output signal recorded at the upper coaxial port with and without groove.

Figure 21: Output signal at the upper coaxial port for a beam with 10.0 mm y-offset.

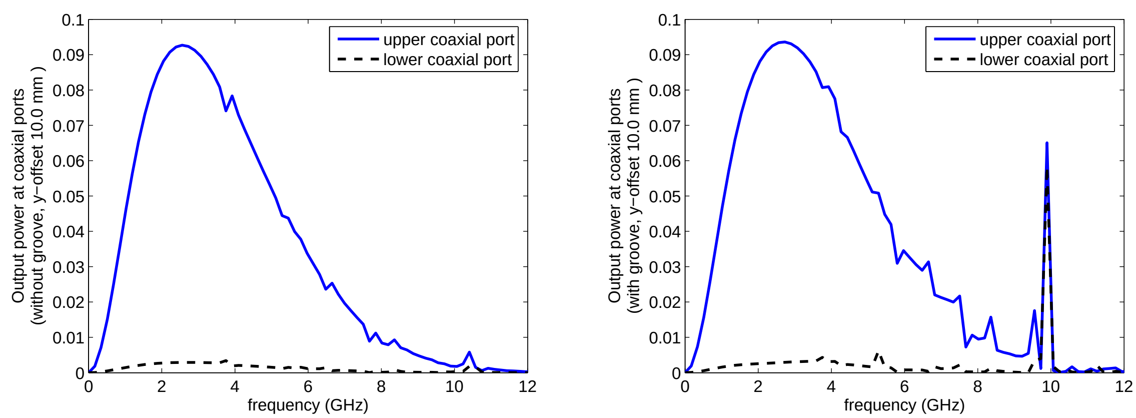

(a) Output signal spectrum at the coaxial ports without groove.

(b) Output signal spectrum at the coaxial ports with groove.

Figure 22: Output signal spectrums at the upper coaxial port for a beam with 10.0 mm y-offset.

Summary

The influences of a beam-pipe discontinuity on the signals of a nearby button type BPM have been studied considering a groove in the beam pipe as discontinuity. The well-known numerical simulation code MAFIA has been used for the computation of the BPM signals. The computation results indicate about 16% deviation of the BPM signal level with and without the discontinuity when it is located 10 mm away from the BPM button. In the case of vertically offset beam, the presence of the discontinuity causes up to 12% deviation in the normalized ratio of the BPM signals. These preliminary studies suggest that a discontinuity near a BPM have a non-negligible influence on its signals. Further studies with different beam-pipe and discontinuity geometries can be helpful to better understand and estimate these effects.

References

[1] "CST Microwave Studio," CST AG, Darmstadt, Germany.

[2] "MAFIA," CST AG, Darmstadt, Germany.

[3] T. Weiland and R. Wanzenberg, "Wakefields and Impedances," in *Proceedings US-CERN School*, M. Dienes, M. Month, S. Turner, Ed. Berlin: Springer-Verlag, 1992.

[4] P. B. Wilson, "High-Energy Electron Linacs: Applications to Storage Ring RF Systems and Linear Colliders," *AIP Conf. Proc.*, vol. 87, pp. 450–555, 1982.

[5] A. K. Bandyopadhyay, A. Jöstingmeier, A. S. Omar, K. Balewski, and R. Wanzenberg, "Wake Computations for the Beam Positioning Monitors of PETRA III," in *Proc. European Particle Accelerator Conference*, Edinburgh, Scotland, 2006.

[6] A. K. Bandyopadhyay, A. Jöstingmeier, A. S. Omar, and R. Wanzenberg, "Wake Computations for Selected Components of PETRA III," *ICFA Beam Dyn. Newslett.*, vol. 45, pp. 147–154, 2008.

[7] ——, "Computations of Wakefields for Beam Position Monitors of PETRA III," 2006, DESY-M-06-02.